Magneto-Optical Investigations of a Novel Superlattice: HgTe-CdTe

Y. Guldner, G. Bastard, J. P. Vieren, and M. Voos
Groupe de Physique des Solides de l'Ecole Normale Supérieure, Laboratoire associé au Centre National de la Recherche Scientifique, 75231 Paris Cedex 05, France

and

J. P. Faurie [a] and A. Million
Laboratoire Infrarouge, LETI-CENG, 38041 Grenoble Cedex, France
(Received 6 June 1983)

Far-infrared magnetoabsorption experiments done in a HgTe-CdTe superlattice are presented. From the results, which are interpreted in terms of interband transitions from valence to conduction subbands, the superlattice band structure has been deduced. These investigations show, in particular, that this superlattice is a quasi zero-energy-gap semiconductor, and yield the first determination of the offset between the HgTe and CdTe valence bands.

PACS numbers: 78.20.Ls, 73.40.Lq, 78.65.Jd

For about the last ten years there has been strong interest in semiconductor superlattices (SL) fabricated from III-V compounds, such as GaAs-$Al_xGa_{1-x}As$ and InAs-GaSb structures for example. Quite recently Faurie, Million, and Piaguet[1] have reported the successful growth by molecular-beam epitaxy (MBE) of a novel system involving II-VI materials, namely HgTe-CdTe superlattices.

We wish to report the first investigations of the electronic properties of a HgTe-CdTe superlattice from far-infrared magnetoabsorption experiments performed at low temperature. The optical transitions observed under magnetic field are interpreted by fitting the data with theoretical calculations done in the envelope-function formalism.[2] These results demonstrate that the structure under investigation is actually a HgTe-CdTe superlattice displaying electronic properties which are found neither in bulk HgTe and CdTe materials, nor in the ternary random alloy $Hg_{1-x}Cd_xTe$. This superlattice is a quasi zero-energy-gap semiconductor, resulting from an accidental band degeneracy. From these studies, we deduce the valence band offset Λ at the HgTe-CdTe interface, and the SL band structure along the growth axis. At a low magnetic field, the electron effective mass in the plane of the layers is strongly nonparabolic and much lighter than in bulk HgTe,[3] an effect due to the peculiar band structure of our superlattice. Finally, with increasing magnetic field, the ground electron subband behavior changes from three-dimensional to two-dimensional, which is a unique feature, also understood from the SL band structure.

Before describing the data, we calculate the band structure of our superlattice, which was grown[1] by MBE on a (111) CdTe substrate and consists of 200 alternate layers of HgTe and CdTe, whose thicknesses are $d_1 = 180$ and $d_2 = 44$ Å, respectively. The band structure of bulk HgTe and CdTe is shown in Fig. 1(a). That of the HgTe-CdTe superlattices has been obtained from two methods, namely the linear combination of atomic orbitals (LCAO) approach[5] and the envelope-function scheme,[2] which is the one used here. A

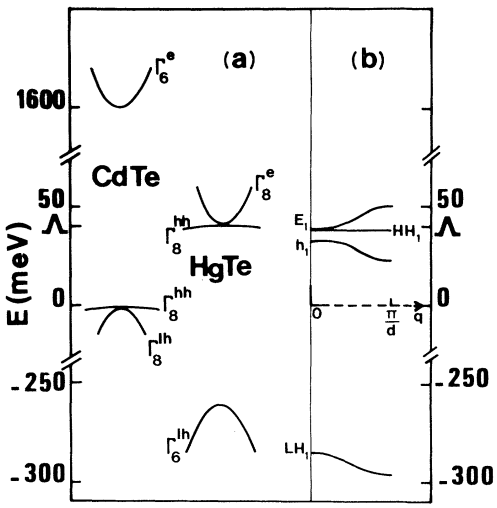

FIG. 1. (a) Band structure of bulk HgTe and CdTe. The e, hh, and lh indices correspond to electrons, heavy holes, and light holes, respectively. (b) Calculated band structure along q of the superlattice under investigation here.

SL state is labeled by a subband index (HH_n, E_n, h_n, ...), a SL wave vector q ($-\pi/d < q < \pi/d$, where d is the SL period), and a two-dimensional wave vector $\vec{k}_\perp$, which is perpendicular to the growth axis z. At $\vec{k}_\perp = 0$, there exists an *exact* decoupling between the heavy-hole states (Γ_8^{hh} in CdTe, Γ_8^{hh} in HgTe), and the light-particle states (Γ_8^{lh} and Γ_6^{e} in CdTe, Γ_8^{e} and Γ_6^{lh} in HgTe). Hall measurements show that the sample is p type for $T \lesssim 20$ K, so that the overlap $\Lambda = E_{\Gamma_8}^{HgTe} - E_{\Gamma_8}^{CdTe}$ is positive; otherwise, charge transfer would occur between CdTe and HgTe, leading to an n-type structure. Hence, for the heavy holes, the CdTe layers act like potential barriers. As shown later from the analysis of the data, $\Lambda \sim 40$ meV and the calculated SL band structure[6] is given in Fig. 1(b), the energy origin being taken at the top of the Γ_8 valence band of CdTe. The ground heavy-hole subband HH_1 is almost dispersionless and is located ~2 meV below the Γ_8 HgTe band edge. The light-particle spectrum is much more intricate. In the energy range of interest ($0 < E < \Lambda$), the relevant bands are Γ_8^{e} in HgTe and Γ_8^{lh} in CdTe. In a first approximation they display the same symmetry (P-like, Γ_8). To get a first hint of the qualitative aspect of the SL light-particle states, we may use a simple plane-wave analysis. The carrier effective mass is positive in HgTe ($\sim 0.03 m_0$) and negative in CdTe ($\sim -0.15 m_0$). One should ensure the conservation of the wave function and of the probability current at the interfaces, including therefore this mass reversal. This leads to a lack of confinement of the ground conduction subband E_1 resulting in a quasi zero-energy-gap structure, as can be seen in Fig. 1(b) which corresponds, of course, to more sophisticated calculations done in the envelope-function approximation. The confinement energy may even vanish or become negative (i.e., $E_1 < \Lambda$) if d is large enough. For $d_1/d_2 \sim 4$, $E_1 < \Lambda$ if $d > 250$ Å. Concomitantly, the E_1 bandwidth ΔE_1 along q drops sharply with increasing d: $\Delta E_1 = 12$ meV for $d = 224$ Å and $\Delta E_1 < 1$ meV for $d > 450$ Å. When E_1 is below HH_1 at $q = 0$, the superlattice is semimetallic, in agreement with Hall measurements done in a (400 Å)HgTe-(150 Å)CdTe SL which show that this structure is n type down to the lowest temperatures used (10 K), while the (180 Å)HgTe-(44 Å)CdTe SL studied here changes from n to p type for $T \sim 20$ K, a well-known behavior in bulk HgTe.[7] Finally, the topmost light-hole subband h_1 [Fig. 1(b)] is always found in the forbidden energy gap $(0, \Lambda)$ for the d_1/d_2 ratio under consideration: For $d = 224$ Å, $h_1(q=0) = 33$ meV and $\Delta h_1 = 10$ meV.

The far-infrared magnetoabsorption experiments reported here were done at 1.6 K using, as infrared sources, a molecular laser and Carcinatrons. The transmission signal, observed at fixed photon energies in the Faraday geometry, was detected by a carbon bolometer. The magnetic field, B, was provided by a superconducting coil and could be varied continuously from 0 to 10 T.

Figure 2 shows typical transmission spectra as a function of B obtained for different infrared wavelengths λ, B being perpendicular to the plane of the layers ($\theta = 0$). Figure 3(a) gives the energy positions of the transmission minima (i.e., absorption maxima) as a function of B from the data presented in Fig. 2. As shown below from quantitative analyses, the observed optical transitions, which are denoted 1-0, 2-1, and 3-2 in Fig. 3(a), correspond to interband transitions at $q = 0$ from HH_1 to E_1 Landau levels. They extrapolate to an energy $h\nu \sim 0$ at $B = 0$, as they should for a quasi zero-gap semiconductor. None of the curves presented in Fig. 3(a) can be due to electron cyclotron resonance because the sample is p type at low temperature. Furthermore, neither can these results be due to hole cyclotron resonance

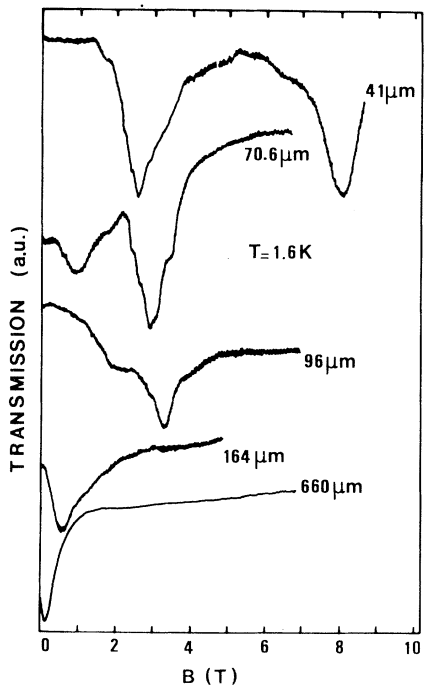

FIG. 2. Typical transmission spectra as a function of the magnetic field for different infrared wavelengths.

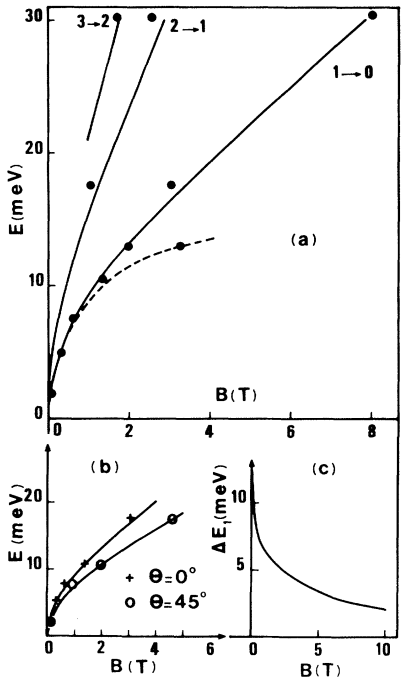

FIG. 3. (a) Position of the transmission minima (see Fig. 2) as a function of the infrared photon energy E and magnetic field (full dots). The solid lines correspond to theoretical fits described in the text. The dashed line is only a guide to the eye emphasizing the deviation between experiment and theory around 2.5 T. (b) Same results for two values of θ (open circles and crosses: experimental data; solid lines: theory) for the transitions 1-0. The solid line for $\theta = 45°$ corresponds to a perfect two-dimensional behavior ($\cos\theta$ law). (c) Calculated width ΔE_1 of the E_1 subband as a function of B for $n = 0$.

because they would yield hole masses which would be much too light. Figure 3(b) gives the same results for $\theta = 0$ and $\theta = 45°$ for the transitions noted 1-0. For $B < 0.3$ T, we observe that the magnetic field position of these transitions is independent of θ, giving evidence for a three-dimensional character. However, for $B > 1$ T, it varies like $(\cos\theta)^{-1}$, which is a two-dimensional behavior in a quasi zero-gap semiconductor.

To be quantitative, we should now calculate the Landau levels of HH_1 and E_1, the Fermi level E_F being close to HH_1 because of the large heavy-hole density of states. For finite $\vec{k}_\perp$ (or finite B), heavy complications occur and are associated with the intricate Γ_8-band kinematics. In particular, the light- and heavy-particle states become $\vec{k}_\perp$ admixed, and we have not been able to overcome all the difficulties induced by the finite $\vec{k}_\perp$. Thus, to obtain the E_1 Landau levels, we have used the approximate SL dispersion relations established previously[2] for finite $\vec{k}_\perp$, neglecting spin effects and replacing $\vec{k}_\perp^2$ by $(2n+1)eB/\hbar$, where $n = 0, 1, \ldots$ is the Landau-level index. The HH_1 Landau-level energies have been taken as dispersionless with q, so that $HH_1(n) = HH_1 - (n+\frac{1}{2})\hbar eB/m_{hh}$, where m_{hh} is the heavy-hole effective mass in bulk HgTe. Our model depends on a single parameter Λ, all the others being well-established bulk parameters. The curves in Figs. 3(a) and 3(b) are theoretical fits to the data using this model. The band gap and hole (electron) effective mass of bulk HgTe are taken equal[3,4] to 0.3025 eV and $0.3m_0$ ($0.03m_0$), respectively, while the band gap of bulk CdTe is 1.6 eV. The curve noted 1-0 corresponds to transitions from the $n = 1$ HH_1 Landau level to the $n = 0$ E_1 Landau level at $q = 0$. The other curves are similar transitions with hole and electron Landau indices which are $n = 2, 3$ and $n = 1, 2$, respectively. Good agreement between experiment and theory is obtained for $\Lambda = (40 \pm 10)$ meV. Note that the experimental data could be interpreted almost as well with the selection rule $\Delta n = +1$, except for the first transition ($1 \to 0$). In particular, the transitions $0 \to 1$ ($1 \to 2$) would practically coincide with the transitions labeled $2 \to 1$ ($3 \to 2$) in Fig. 3(a), since most of the transition energies arise from the conduction levels. Another feature emerges from these fits, namely, the strong nonparabolicity of the E_1 Landau levels, whose apparent effective mass increases from $8 \times 10^{-3} m_0$ (low field) towards the value of the electron effective mass of bulk HgTe[4] ($0.03m_0$) at high field. We have also calculated the width ΔE_1 of the E_1 subband as a function of B for $n = 0$. The results are given in Fig. 3(c), and they show that ΔE_1 decreases rapidly with B, which can explain the observed change from three-dimensional to two-dimensional behavior. We believe that the very light SL transverse mass of the E_1 subband found at low field reflects the strong $\vec{k}\cdot\vec{p}$ interaction between the E_1, HH_1, and h_1 subbands which are very close at $q = 0$ [Fig. 1(b)]. On the other hand, from our calculations, E_1 and HH_1 (h_1) are 13 (28) meV apart at $q = \pi/d$ and $B = 0$ which, along the same interpretation, leads to slower upward shift of E_1 at $q = \pi/d$ than at $q = 0$, explaining the decrease of ΔE_1 with increasing B. In addition, one can see that the experimental data for the 1-0 transition deviate from the theoretical fit in Fig. 3(a) for $B \sim 2.5$ T and for an energy ~ 15 meV. This is likely to be due to an interband polaron

effect since the LO-phonon energy is 16 meV in bulk HgTe.

Finally, we have also done magnetoabsorption experiments at higher energy (300–400 meV) to trace back the SL subband LH_1 derived from the $\Gamma_6{}^{1h}$ HgTe states (Fig. 1). In fact, the energy of the observed transitions as a function of B extrapolates to 340 meV at $B=0$. They correspond to interband transitions between Landau levels of LH_1 and E_1 [Fig. 1(b)], since the band gap between LH_1 and E_1 at $q=0$ is, from our calculations, equal to 325 meV. Besides, the slope of the observed transition energies versus B are very well interpreted by our model. These observations rule out appreciable interdiffusion between HgTe and CdTe layers because, in the resulting $Hg_xCd_{1-x}Te$ alloy, the corresponding band gap would be *smaller* than 302.5 meV, its value[4,8] in bulk HgTe. Interdiffusion can also be discarded from the results shown in Fig. 3. This is evident for non-zero-gap $Hg_xCd_{1-x}Te$, and zero-gap $Hg_xCd_{1-x}Te$ would lead[8] to a different nonparabolicity effect.

This work was supported in part by the Direction des Recherches et Etudes Techniques.

[a]Present address: University of Illinois, Chicago, Ill. 60680.

[1]J. P. Faurie, A. Million, and J. Piaguet, Appl. Phys. Lett. 41, 713 (1982).

[2]G. Bastard, Phys. Rev. B 25, 7584 (1982).

[3]J. Tuchendler, M. Grynberg, Y. Couder, H. Thomé, and R. Le Toullec, Phys. Rev. B 8, 3884 (1974).

[4]Y. Guldner, C. Rigaux, M. Grynberg, and A. Mycielski, Phys. Rev. B 8, 3875 (1973).

[5]J. N. Schulman and T. C. McGill, Appl. Phys. Lett. 34, 663 (1979), and Phys. Rev. B 23, 4149 (1981).

[6]Detailed calculations will be published elsewhere.

[7]See, e.g., B. L. Gelmont, M. I. Dyakonov, V. I. Ivanov-Omskii, B. T. Kolomiets, V. K. Ogorodnikov, and K. P. Smekalova, in *Proceedings of the Eleventh International Conference on the Physics of Semiconductors, Warsaw, 1972*, edited by the Polish Academy of Sciences (PWN—Polish Scientific Publishers, Warsaw, 1972), p. 938.

[8]Y. Guldner, C. Rigaux, A. Mycielski, and Y. Couder, Phys. Status Solidi (b) 81, 615 (1977), and 82, 149 (1977); R. S. Kim and S. Narita, Phys. Status Solidi (b) 73, 741 (1976).